Ecotoxicology and Public Health

Perfluoroalkyl Substances Stimulate Insulin Secretion by Islet # Cells via G Protein-Coupled Receptor 40

Wei-Ping Qin, Lin-Ying Cao, Chuan-Hai Li, Liang-Hong Guo, John K Colbourne, and Xiao-Min Ren

Environ. Sci. Technol., **Just Accepted Manuscript** • DOI: 10.1021/acs.est.9b07295 • Publication Date (Web): 24 Feb 2020

Perfluoroalkyl Substances Stimulate Insulin Secretion by Islet β Cells via G Protein-Coupled Receptor 40

Wei-Ping Qin[a], Lin-Ying Cao[a], Chuan-Hai Li[a], Liang-Hong Guo[b]*, John Colbourne[c], Xiao-Min Ren[a]*

[a] State Key Laboratory of Environmental Chemistry and Eco-toxicology, Research Center for Eco-environmental Sciences, Chinese Academy of Sciences, 18 Shuangqing Road, Beijing 100085, China

[b] Institute of Environmental and Health Sciences, China Jiliang University, Hangzhou, Zhejiang 310018, China

[c] School of Biosciences, University of Birmingham, Edgbaston, Birmingham B15 2TT, UK

***Corresponding authors:**

Liang-Hong Guo, Institute of Environmental and Health Sciences, China Jiliang University, Hangzhou, Zhejiang 310018, China. Telephone/Fax: 86-0571-86876235, E-mail: LHGuo@cjlu.edu.cn.

Xiao-Min Ren, State Key Laboratory of Environmental Chemistry and Eco-toxicology, Research Center for Eco-Environmental Sciences, Chinese Academy of Sciences, 18 Shuangqing Road, Beijing 100085, China. Telephone: 86-010-62849338, Email: xmren@rcees.ac.cn.

ABSTRACT

The potential causal relationship between exposure to environmental contaminants and diabetes is troubling. Exposure of perfluoroalkyl substances (PFASs) is found to be associated with hyperinsulinemia and the enhancement of insulin secretion by islet β cells in humans, but the underlying mechanism is still unclear. Here, by combining *in vivo* studies with both wild type and gene knockout mice and *in vitro* studies with mouse islet β cells (β-TC-6), we demonstrated clearly that one-hour exposure of perfluorooctane sulfonate (PFOS) stimulated insulin secretion and intracellular calcium level by activating G protein-coupled receptor 40 (GPR40), a vital free fatty acid regulated membrane receptor on islet β cells. We further showed that the observed effects of PFASs on mouse model may also exist on human by investigating the molecular binding interaction of PFASs with human GPR40. We thus provided evidence for a novel mechanism for how insulin-secretion is disrupted by PFASs in human.

Key Words: perfluoroalkyl substances; GPR40; insulin secretion; intracellular calcium; islet β cells

42 **A graphic for the Table of Contents**

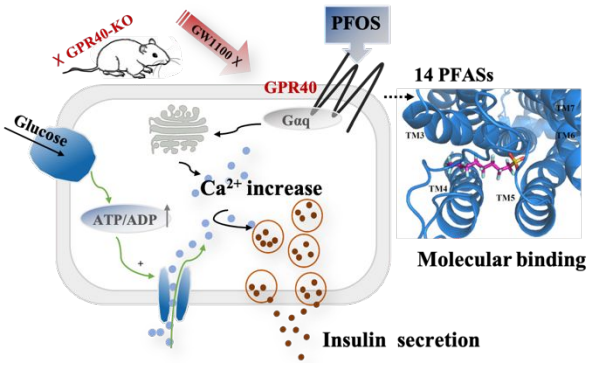

43

INTRODUCTION

Perfluoroalkyl substances (PFASs) are a class of persistent organic pollutants with great threat to environmental and human health. Perfluorooctane sulfonate (PFOS) is one of the most concerned members of PFASs. It was detected in the serum of the general public at concentrations around 0.05 μg/mL (0.1 μM)[1], while the concentrations for occupationally exposed workers were recorded to exceed 10 μg/mL (20 μM)[2]. Although strict global regulation has restricted the production and usage of PFOS[3,4], human exposure to PFOS will persist for many years since the half-life of PFOS is around 5.4 years in the human body[5]. In addition, many other PFASs including perfluoroalkyl carboxylic acids have also been detected in various environmental media, wildlife and humans[1,6,7]. Their levels are expected to increase over time since they are not yet listed in the Stockholm Convention.

Recently, the relationship between PFASs and diabetes has gained great concerns[8-11]. Insulin level is a crucial indicator for diagnosis of diabetes. Many epidemiological investigations demonstrated significant positive associations between PFOS and perfluorooctanoic acid (PFOA) exposure with β cell function, insulin resistance, fasting proinsulin and insulin levels[12-15]. For example, Lin et al. found that, according to the data from NHANES 1999-2000 and 2003-2004, the increased serum PFOS level was accompanied with higher fasting insulin level and higher insulin secretion activity of β cells among U.S adolescents and adults[13]. More specific data indicated that an increase of serum PFOS concentration by 10 ng/mL was associated with 16% rise of serum insulin level and 12% increase of β cells insulin secretion activity among overweight

children in a subset of the European Youth Heart Study[14].

Reasons for the abnormal serum insulin level may be complex, which may include disruptive insulin secretion function of pancreas as well as the abnormal insulin response function of hepatic or adipose tissue[16]. Previous toxicological studies of PFASs on experimental animals mainly focused on the hepatic and adipose tissues[17-23]. However, metabolic regulations in these tissues are downstream responding signal pathways of insulin. Pancreas is the only known organ to release insulin[24], but few studies have been performed on this upstream regulation. PFOS has been detected in the pancreatic tissue of human[25], indicating that PFOS can reach human β cells. It is therefore reasonable to speculate that the insulin disorder associated with PFASs exposure may be due to the dysfunction of β cells. Unfortunately, up to now studies on the effects of PFASs on pancreas β cells are limited to the adverse effects on pancreas organogenesis in mice and zebrafish, without a clear mechanism[26-28].

G protein-coupled receptor 40 (GPR40) - also known as the free fatty acid receptor 1 (FFAR1) - is highly expressed on the membrane of islet β cells[29]. GPR40 can be activated by medium- and long-chain free fatty acids (FFAs), leading to the increase of intracellular calcium level and the secretion of insulin[29,30]. Previous studies demonstrated that PFASs could mimic the functions of FFAs due to their structural similarity. PFASs were showed to bind with and activate peroxisome proliferator-activated receptors (PPARs) and affect the cellular functions regulated by these receptors[31,32]. We therefore speculate that PFASs could also activate GPR40 in β cells and stimulate insulin secretion. However, other studies have also demonstrated that

structure-based predictions are not reliable. For example, PFASs are structurally very different from thyroid hormones (T_3, T_4) and estrogens (17β-estradiol), and yet they have been shown to activate thyroid hormone and estrogen receptors[33-36]. Therefore, experimental verification for the predicted PFOS effects on GPR40 is vital.

In this study, we investigated and verified the role of GPR40 in the PFOS effects on insulin secretion activity of β cells by using a combined approach of *in vivo*, *in vitro* and *in silicon* experiments. We also investigated the interaction of PFOS with human GPR40 so as to provide support for our assumption that the mechanism revealed in the mouse model might also exist in humans. In addition, the binding interaction of 14 other PFASs with GPR40 was investigated to assess their potential effects on the insulin secretion activity of β cells via GPR40.

EXPERIMENTAL SECTION

Reagents. 15 PFASs (purity ≥ 98%) used in this study are listed in the Table 1 and their full names and structures are shown in the Table S1. 3 PFASs (PFOS, PFHxDA and PFOcDA) were purchased from Alfa Aesar (USA). Other 12 PFASs (PFBA, PFBS, PFHxA, PFHxS, PFHpA, PFOA, PFNA, PFDA, PFUnA, PFDoA, PFTriDA, PFTeDA) were purchased from Sigma (USA). Lauric acid (LA, purity ≥ 98%) and GW1100 (purity ≥ 97%) were purchased from Sigma-Aldrich (USA). TAK-875 (purity ≥ 99%) was purchased from Selleckchem (USA). All the chemicals were dissolved in DMSO and stocked in -20 °C.

Animal Treatments. C57BL/6 (6-7 weeks old) mice were purchased from Beijing

Vital River Laboratory (China). GPR40 knock out (GPR40-KO) C57BL/6 mice were constructed by Beijing Biocytogen (China). After 12-hour fasting, mice were weighted by an electronic balance and administered 0, 0.5, 1, 5 and 10 mg PFOS per kilogram body weight by gavage[21,37]. After one hour, mouse serum was collected for insulin detection by ultrasensitive insulin ELISA kit (Mercodia, Sweden). All the experimental operations were carried out according to the institutional guidelines for the care and use of laboratory animals. The details of operation process are shown in the supporting information.

Cell lines and culture condition. Mouse islet β cancer cells (β-TC-6) and human embryonic kidney 293 cells (HEK293) were purchased from Shanghai Cell Bank of Chinese Academy of Sciences. β-TC-6 cells were maintained in high glucose Dulbecco's modified Eagle's medium (DMEM, Invitrogen, USA) supplemented with 20% fetal bovine serum (FBS, HyClone, USA), 100 U/mL penicillin and 100 μg/mL streptomycin (Invitrogen, USA). HEK293 cells were cultured in DMEM supplemented with 10% FBS, 100 U/mL penicillin and 100 μg/mL streptomycin. All the cells were cultured at 37°C in a humidified 5% CO_2 atmosphere. GPR40 protein is highly expressed in β-TC-6 cells, while undetectable in HEK293 cells (https://www.proteinatlas.org). β-TC-6 cells were used to verify the insulin-secretion disruption of PFOS on β cells and explore its mechanism underlying this biological effect. HEK293 was used to exogenously express human GPR40 protein by transient transfection, which then was applied for studying the binding effects of chemicals with human GPR40 protein. HEK293 transfected with flag plasmid served as blank control.

Detection of Insulin Secretion Activity of β Cells. β-TC-6 cells (3×10^5 cells/mL) were seeded in 24-well plates and allowed to adhere for 48 hours. Cells were changed into Krebs-Ringer bicarbonate HEPES buffer (KRBH, Leagene, China) with or without 0.1% bovine serum albumin (BSA) for 30 min. Then, the supernatant was removed and replaced by new assay buffer containing different concentration of glucose (Sigma, USA) and tested chemicals in KRBH buffer (with or without 0.1% BSA) for 60 min[38]. Next, the supernatant of each well was collected into a new tube separately; cells that adhered on the bottom of each well were lysed by RIPA (Solarbio, China) for 20 min and then the cell lysate of each well was collected into another tube. Finally, the insulin level of supernatant or cell lysate was detected separately by the rat/mouse insulin ELISA kit (Milipore, USA) after dilution into the detection range; the protein content of cell lysate was quantified by a BCA protein assay kit (Beyotime, China). The detail of operation process is shown in the supporting information.

Detection of the Intracellular Calcium Level of β-TC-6 Cells. Intracellular calcium was detected by using a fluorescence indicator Fura-2AM (Invitrogen, USA)[39]. β-TC-6 cells were harvested and incubated with 5 μM Fura-2 AM and 0.05% pluronic acid (Invitrogen, USA) in phenol-free DMEM at 37 °C for 30 min. Cells were washed twice and incubated for another 30 min in phenol-free DMEM. Cells were re-suspended in phenol-free DMEM at a density of 1×10^7 cells/mL. Then, 10 μL harvested cells were mixed uniformly in 90 μL Hank's balanced salt solution buffer (HBSS, Invitrogen, USA). Next, the intracellular calcium signal was determined by a Horiba Fluoromax-4 Spectrofluorometer (Edison, USA) before and after exposure of tested chemicals. The

detail of information is shown in the supporting information.

Human GPR40 Fluorescence Competitive Binding Assay. The binding affinities of PFASs with human GPR40 (NM_005303) were measured by using a fluorescence competitive binding assay according to our previous work[40]. Briefly, HEK293 cells were transfected with GPR40 plasmid by using lipofectamine 3000 transfection reagent (Life Technologies, USA). After 48 hours, cells were harvested in phenol-free DMEM (1×10^6 cells/mL) and kept on ice. Then, 50 μL harvested cells, 100 nM F-TAK-875A (a specific GPR40 fluorescence probe) and one of tested compounds (TAK-875, LA or PFASs) were mixed in phosphate buffered saline (PBS) buffer in a total volume of 500 μL. After incubation for 2 min at 37°C, the fluorescence signal of cells in the fluorescein isothiocyanate (FITC) channel for each sample was detected by NovoCyte flow cytometer (ACEA Biosciences, USA). At least 10,000 cells were analyzed according to the forward scatter and side scatter. Percentage values of special binding region of ligands to GPR40 were fitted with a sigmoidal model (Origin Lab, USA) to calculate the half-inhibitory concentration (IC_{50}). The relative binding affinity (RBA) compared with LA of each PFASs was obtain by dividing the IC_{50} value with that of LA.

Molecular Docking Simulation. The binding interaction between PFASs and human GRP40 was simulated by Autodock Vina v1.1.2 (San Francisco, USA). A crystal structure of human GPR40 (4PHU) was extracted from the RCSB Protein Data Bank (http://www.rcsb.org/pdb). The docking process was similar to our previous work[40]. Rigid docking mode was used to simulate the binding pattern of tested compounds with human GPR40 at the TAK-875 binding pocket in crystal complex. For

each complex, 10 independent docking runs were conducted, and the binding mode with the lowest binding energy was chosen for comparison.

Statistical Analysis. The results of experiment were analyzed by Microsoft Excel and SPSS software. Data were represented as means ± standard deviation ($n \geq 3$). Differences between two treatment groups were evaluated by student's *t* test. The comparisons among more than two groups were evaluated by two-way analysis of variance (ANOVA). Results were considered as statistically significant if the *p* value < 0.05.

RESULTS AND DISCUSSION

PFOS Stimulates Insulin Secretion of Male Mice via GPR40. We aimed to investigate whether PFOS stimulates insulin secretion by β cells *in vivo*. After administrating 10 mg/kg PFOS for one hour, the fasting serum insulin level of wild type (WT) male mice (0.9 ± 0.5 ng/mL, n = 5) was significantly ($p < 0.05$) higher than that of solvent control group (0.2 ± 0.1 ng/mL, n = 5). However, no difference was observed ($p > 0.05$) between the PFOS treated group and the control group among the female mice (Figure 1A). The sex-biased effect of PFOS on mice is likely due to the protective effect of female estrogen levels, which protects pancreatic β cells against exogenous stimulation and injuries via interacting with estrogen receptors (ERs) and G-protein estrogen receptor (GPER)[41-43]. Xing *et al*. reported that the concentration of PFOS in mouse serum was around 200 μg/mL after treatment with 10 mg/kg/d PFOS for 30 days[37], which was about twenty folds higher than that in human. In order to

198 reveal the toxicological mechanism of tested compounds within a short-term exposure,
199 we used 10 mg/kg PFOS for one-time gavage in our experiment, and this exposure dose
200 showed a stimulated insulin secretion effect on male mice.

201 To examine whether GPR40 is involved in the PFOS induced effect, we also
202 employed GPR40-KO mice in our study. As shown in Figure 1B, there was no
203 significant difference ($p > 0.05$) in the fasting serum insulin level between the 10 mg/kg
204 PFOS treated group (0.5 ± 0.2 ng/mL, n = 6) and the control group (0.4 ± 0.2 ng/mL, n
205 = 7) for the male mice. No obvious difference ($p > 0.05$) was observed between PFOS
206 treated group (0.6 ± 0.1 ng/mL, n = 4) and control group (0.4 ± 0.2 ng/mL, n = 4) among
207 the female GPR40-KO mice (Figure 1B) neither. The above results suggested that
208 short-term administration of PFOS stimulated insulin secretion by β cells in the male
209 mice and that GPR40 might be involved in producing this effect.

210 **PFOS Enhances Insulin Secretion Activity and Intracellular Calcium Level**
211 **of β Cells via GPR40.** To further investigate the effect of PFOS on the insulin secretion
212 activity of β cells, we detected the insulin level of supernatant on the glucose-stimulated
213 insulin secretion (GSIS) by using mouse β-TC-6 cells *in vitro*. In previous studies,
214 KRBH buffer with BSA was used in the GSIS experiment[29,44-46]. BSA is a common
215 protein used in cell related experiments. It can increase cell adhesion and prevent
216 mechanical damage. In addition, BSA is also a good carrier which can bind small
217 molecules such as water, salt and hormones to strengthen cell-to-cell communication[47].
218 Therefore, in our GSIS experiment, KRBH buffer with 0.1% BSA was also used
219 initially to keep in line with the previous studies. Our results showed that 1.4 mM

glucose had the highest activity in the GSIS of β-TC-6 cells with 1.7-fold higher than the control group (Figure S7A). This result was consistent with a previous study showing that β-TC-6 cells were more sensitive to 1.4 mM glucose[38].

In the presence of 1.4 mM glucose, one-hour treatment of 50 μM or 100 μM PFOS enhanced the secretion of insulin by 2.8 or 3.7 folds respectively by comparison with the control group (Figure 2A, 1.4 mM glucose with 0.1% BSA). Since it has been previously demonstrated that BSA can bind with PFOS[48-50], this binding effect might reduce the concentration of free PFOS. KRBH buffer without BSA was used when we studied the insulin-secretion disruption effects of PFASs. Our results showed that the enhancement was further amplified by removing BSA from the KRBH buffer in the GSIS experiment. Compared with the control, 50 μM or 100 μM PFOS enhanced the GSIS of 1.4 mM glucose by 8.3 or 10.6 folds respectively (Figure 2A, 1.4 mM glucose, without BSA). Moreover, the lowest observed effect concentration (LOEC) was lowered from 50 μM to 5 μM when BSA was removed (Figure 2A). We also detected the intracellular insulin content of β-TC-6 cells after the treatment of PFOS. The result of this experiment showed that the enhancement of GSIS by PFOS induction was unassociated with a change of intracellular insulin content (Figure S7B).

The insulin secretion stimulation effect of PFOS was further demonstrated by determining the upstream signal – intracellular calcium[51]. The increase of intracellular calcium levels promotes the fusion of insulin-containing vesicles to plasma, resulting in the secretion of insulin[52]. Therefore, the change of intracellular calcium levels in β-TC-6 cells after PFOS exposure could be used to prove that PFOS disrupts insulin

242 secretion function of β-TC-6 cells. As shown in Figure 2B, in the presence of 1.4 mM
243 glucose, addition of PFOS triggered an increase of intracellular calcium level in β-TC-6
244 cells in a concentration-dependent manner with a LOEC of 5 μM. Combining these
245 above results, we demonstrated that PFOS enhanced the insulin secretion activity of β-
246 TC-6 cells by triggering the increase of intracellular calcium level.

247 Insulin secretion of β cells is mainly regulated by the serum glucose level through
248 the GSIS pathway[53]. We also investigated the effects of different concentration of
249 glucose on the enhancement of PFOS on β-TC-6 cells. As shown in Figure 2C, 50 μM
250 PFOS was sufficient to stimulate the insulin secretion by β-TC-6 cells in the absence
251 of glucose. Compared with the effect induced by 50 μM PFOS alone, co-exposure of
252 1.4 mM or 5.5 mM glucose with PFOS resulted in more insulin secretion by 2.1 or 1.9
253 folds respectively, while 11.1 mM glucose did not (Figure 2C). The intracellular
254 calcium level induced by PFOS in the absence or present of glucose showed a
255 correspondence with the insulin secretion activities of β-TC-6 cells (Figure 2D). Our
256 results showed that PFOS activates the β-TC-6 cells in a glucose-sensitive manner.

257 In the present study, we aimed to reveal the possible mechanism for the PFOS
258 induced insulin secretion effect of β cells. Two GPR40 agonists (TAK-875[54] and LA[55])
259 and one GPR40 antagonist (GW1100[56]) were used to investigate whether GPR40 is
260 involved in the effect of insulin secretion stimulation activity of PFOS on β-TC-6 cells.
261 TAK-875 and LA also enhanced the GSIS and trigger the intracellular calcium increase
262 of β-TC-6 cells in a concentration-dependent manner (Figure S8). When the β-TC-6
263 cells were pre-incubated with 10 μM GW1100, GSIS induced by TAK-875 or LA was

264 significantly ($p < 0.05$) inhibited by 63% or 88% respectively. Similar to these two
265 GPR40 agonists, the enhancement of GSIS induced by 50 μM PFOS was also inhibited
266 by 49% (Figure 2E). With the addition of 10 μM GW1100, the intracellular calcium
267 levels also declined when compared with the cells exposed to TAK-875, LA and PFOS
268 only (Figure 2F). These results suggested that the interaction of PFOS with mouse
269 GPR40 is a possible molecular initiating event for its effects on mouse β cells. So far,
270 our work on mice and mouse-derived cell lines has firstly identified GPR40-mediated
271 pathway as a likely mechanism of PFOS disruption on insulin secretion.

272 **Studying the Interaction of PFOS with Human GPR40.** The demonstrated
273 interaction of PFOS with mouse GPR40 can in principle be the molecular event that
274 initiates the observed effects of PFOS on mouse β cells. However, due to significant
275 species differences, this mechanism cannot be extrapolated directly to humans to
276 provide causal linkage between PFOS exposure and health effects. We therefore studied
277 this likely interaction of PFOS with human GPR40 by quantitatively determining its
278 binding affinity with human GPR40 and computationally simulating its interaction with
279 this receptor.

280 HEK293 cells originate from human without GPR40 expression. After transient
281 transfection for 48 hours, HEK293 cells exogenously expressed human GPR40 protein,
282 which was used to study the binding effects of PFOS with human GPR40. We
283 employed a competitive binding assay previously established in our lab[40], which used
284 a specific fluorescent probe F-TAK-875A designed on the basis of the crystal structure
285 of human GPR40/TAK-875 complex[57]. As the concentration of LA (used as a positive

286 control) increased, more fluorescent probes were displaced from human GPR40,
287 indicating the binding of LA to human GPR40 (Figure 3A). Using this assay, PFOS
288 similarly displaced the probe from human GPR40 in a concentration-depended manner
289 (Figure 3A), suggesting that PFOS also binds with human GPR40. By comparing the
290 IC_{50} value of PFOS (4.4 μM) with that of LA (7.4 μM), we discovered that PFOS had
291 1.7-fold greater binding potency than LA.

292 The result of the molecular docking also supported our finding that PFOS binds
293 with human GPR40. LA was docked into the human GPR40 with its carboxylic acid
294 substituent targeting the inner part of the receptor and forming hydrogen bonds with
295 arginine (Arg) 183, tyrosine (Tyr) 2240, while with its carbon chain being positioned
296 towards the entrance of the binding pocket (Figure 3C). PFOS was docked into human
297 GPR40 with the same binding mode as LA (Figure 3B), with its sulfonic acid
298 substituent targeting the inner part of human GPR40 and forming hydrogen bonds with
299 Arg 183, Tyr 2240, and Arg 2258, while with its carbon chain being positioned towards
300 the entrance of the binding pocket (Figure 3D). This is a sensible result since they have
301 similar chemical structures. Some previous studies based on molecular docking also
302 showed PFOS and LA had similar binding mode in the nuclear receptors of FFAs, for
303 example PPARs[31,32]. Based on the above results, we demonstrated that PFOS binds
304 with human GPR40, which might be the initiating event for the insulin-secretion
305 disruption effect of human β cells.

306 Previously, several epidemiological studies showed that the serum PFOS level was
307 positive associated with hyperinsulinemia (higher fasting serum insulin level) in

human[11-14]. For occupationally exposed workers, serum PFOS concentrations were reported to be in the range of 1 μM to 20 μM[2]. In the present study, we found that 5 μM PFOS was sufficient to enhance the GSIS and increase the intracellular calcium level of β-TC-6 cells (Figure 2A-B). Moreover, based on the human GPR40 competitive binding assay, 5 μM PFOS binds with human GPR40 (Figure 3A). These results suggested a possible risk of PFOS for some occupational workers with up to micromolar serum PFOS concentrations. Thus, our study provided a possible mechanism for this observed insulin-secretion disruption effect of PFOS in human, which is by interacting with the GPR40 on the human β cells.

Predicting the insulin-secretion disruption risks of other PFASs via the GPR40 pathway. Considering the structural similarity of other PFASs with PFOS, the effects induced by PFOS are likely shared with other PFASs[31,32,58,59]. We therefore predicted the risk of insulin-secretion disruption caused by other 14 PFASs on β cells by studying their interactions with human GPR40 using competitive binding assay and molecular docking.

As shown in Table 1, Figure 4A-B and Figure S9, among these tested PFASs, 6 compounds (PFHxS, PFOA, PFNA, PFDA, PFUnA and PFDoA) can also bind with human GPR40 with IC_{50} values ranging from 167.7 μM to 0.7 μM. Compared with LA (setting the binding affinity of LA with human GPR40 as 1), PFDA [with relative binding affinity (RBA) of 1.5], PFUnA (RBA=2.6) and PFDoA (RBA=10.6) had higher binding affinity with human GPR40. However, the IC_{50} values could not be obtained for the PFASs compounds with the alkyl chain length less than 6 carbons (Table 1). As

the length of alkyl chain increases from 7 carbons to 11 carbons, the RBA increased from 0.1 to 10.6 (Table 1). The RBA of the compounds with chain length greater than 11 carbons did not excess this maximum value (Table 1). In addition, we found that PFOS (RBA = 1.7) had much higher binding affinity than PFNA (RBA = 0.3), which have the same length of fluorinated alkyl chain but with different substituents. These results demonstrated that the binding affinity of the PFASs to GPR40 is dependent on the alkyl chain length and the terminal acid group of PFASs, which is similar to the dependence observed for the binding affinity of PFASs with other proteins, such as PPARs[32], ERs[36], thyroid hormone receptor[33], transthyretin[60], and fatty acid binding protein[59].

The docking results also well explained the relationship between the binding affinity and the alkyl-chain length. 14 PFASs fitted within the ligand binding pocket of human GPR40 with similar binding geometry as LA (Figure 3B, Figure 4C-D and Figure S10). All of their sulfonic or carboxylic acid substituents were oriented towards the inner part of GPR40 and formed hydrogen bonds with Arg 183, Tyr 2240, or Arg 2258 (Table 1). Their hydrophobic fluorinated alkyl chains were positioned towards the entrance of the binding pocket. However, their exact binding geometry was slightly different from each other. For the PFASs with chain length shorter than 11 carbons, they were enclosed within the binding core of the receptor (Figure 4C-D and Figure S10). As the chain length increased, hydrophobic interaction between PFASs and GPR40 also increased, leading to higher binding affinity. For the PFASs with chain lengths longer than 11 carbons, their molecular sizes were larger than the volume of the

352 ligand binding pocket. The acid end group and neighboring fluorinated alkyl moiety of
353 the long-chain PFASs occupied the binding core fully, while the remaining alkyl chain
354 extended outside the binding pocket (Figure S10). This may destabilize the binding
355 between PFASs and human GPR40. This dependency of binding affinity on carbon-
356 chain length is in good accordance with our previous study on the binding affinity of
357 18 FFAs (C5- C23) with human GPR40[40]. The above results obtained from the
358 competitive binding assay and molecular docking demonstrated that some PFASs other
359 than PFOS could also bind to human GPR40, suggesting the possibility of the
360 disruption effect of these PFASs on the insulin secretion activity of β cells.

361 To evaluate the predictability of the above GPR40 binding results for the potential
362 insulin-secretion disruption of PFSAs, we then investigated their effects on GSIS of β
363 cells. It is better to carry out this study by using human origin β cells, but this cell line
364 is not available for us currently. β-TC-6 cell line that endogenously expresses mouse
365 GPR40 can be a good alternative. PFOA (the most commonly found PFAS in the
366 environment) and PFDoA (having the greatest human GPR40 binding affinity
367 according to our study) were tested. Our results show that both PFOA and PFDoA
368 enhanced the insulin secretion by β-TC-6 cells (Figure 4E-F). In the presence of 1.4
369 mM glucose, the treatment of 50 μM or 100 μM PFOA enhanced the secretion of insulin
370 by 1.5 or 1.6 folds respectively, and the treatment of 10 μM or 20 μM PFDoA enhanced
371 the secretion of insulin by 1.4 or 1.6 folds respectively. Our results suggested that, in
372 addition to PFOS, the potential disruption effect of other PFASs to the insulin secretion
373 activity of β cells (possibly in humans) should not be ignored.

374

375 **Notes**

376 The authors declare no competing financial interest

377

378 **Acknowledgement**

379 This work was supported by the Chinese Academy of Sciences (QYZDJ-SSW-
380 DQC020), National Natural Science Foundation of China (91543203, 21777187), and
381 the Royal Society International Collaboration Award for Research Professors
382 (IC160121).

383

384 **Supporting Information**

385 The Supporting Information is available free of charge on the ACS Publications
386 website. Detail information of detection of serum insulin levels of C57BL/6 mice,
387 detection of insulin secretion activity and intracellular calcium level of β-TC-6 cells.
388 Results of the active effects of glucose, PFOS, TAK-875 and lauric acid on β-TC-6
389 cells, results of competitive binding curves and molecular docking of 12 PFASs with
390 human GPR40.

391

392 **Reference**

393 1. Yeung, L. W., So, M. K., Jiang, G., Taniyasu, S., Yamashita, N., Song, M., Wu,
394 Y., Li, J., Giesy, J. P., Guruge, K. S. & Lam, P. K. Perfluorooctanesulfonate and
395 related fluorochemicals in human blood samples from China. *Environ. Sci.*
396 *Technol.* **40**, 715 (2006).
397 2. Alexander, J., Auounsson, G. A. & Benford, D. Perfluorooctane sulfonate (PFOS),
398 perfluorooctanoic acid (PFOA) and their salts scientific opinion of the panel on
399 contaminants in the food chain. *Efsa Journal* **653**, 1-131 (2008).
400 3. Laura, H., Alastair, I. & Rachel, M. F. Litigating toxic risks ahead of regulation:
401 biomonitoring sience in the courtroom. *Stanf. Environ. Law. J.* **31,** 3 (2012).
402 4. Wang, T., Wang, Y., Liao, C., Cai, Y. & Jiang, G. Perspectives on the inclusion of
403 perfluorooctane sulfonate into the Stockholm Convention on persistent organic
404 pollutants. *Environ. Sci. Technol.* **15**, 5171–5175 (2009).
405 5. Olsen, G. W., Burris, J. M., Ehresman, D. J., Froehlich, J. W., Seacat, A. M.,
406 Butenhoff, J. L. & Zobel, L. R. Half-life of serum elimination of
407 perfluorooctanesulfonate, perfluorohexanesulfonate, and perfluorooctanoate in
408 retired fluorochemical production workers. *Environ. Health Perspect.* **115**, 1298-
409 1305 (2007).
410 6. Seo, S. H., Son, M. H., Shin, E. S., Choi, S. D. & Chang, Y. S.Matrix-specific
411 distribution and compositional profiles of perfluoroalkyl substances (PFASs) in
412 multimedia environments. *J. Hazard Mater.* **364**, 19-27 (2019).
413 7. Zafeiraki, E., Gebbink, W. A., Hoogenboom, R. L. A. P., Kotterman, M., Kwadijk,

C., Dassenakis, E. & van Leeuwen, S. P. J. Occurrence of perfluoroalkyl substances (PFASs) in a large number of wild and farmed aquatic animals collected in the Netherlands. *Chemosphere* **232**, 415-423 (2019).

8. MacNeil, J., Steenland, N. K., Shankar, A. & Ducatman, A. A cross-sectional analysis of type II diabetes in a community with exposure to perfluorooctanoic acid (PFOA). *Environ. Res.* **109**, 997-1003 (2009).

9. Taylor, K. W., Novak, R. F., Anderson, H. A., Birnbaum, L. S., Blystone, C., Devito, M., Jacobs, D., Köhrle, J., Lee, D. H., Rylander, L., Rignell-Hydbom, A., Tornero-Velez, R., Turyk, M. E., Boyles, A. L., Thayer, K. A. & Lind, L. Evaluation of the association between persistent organic pollutants (POPs) and diabetes in epidemiological studies: A national toxicology program workshop review. *Environ. Health Perspect.* **121**, 774-783 (2013).

10. Lind, L., Zethelius, B., Salihovic, S., van Bavel, B. & Lind, P. M. Circulating levels of perfluoroalkyl substances and prevalent diabetes in the elderly. *Diabetologia.* **57**, 473-479 (2014).

11. Wang, H., Yang, J., Du, H., Xu, L., Liu, S., Yi, J., Qian, X., Chen, Y., Jiang, Q. & He, G. Perfluoroalkyl substances, glucose homeostasis, and gestational diabetes mellitus in Chinese pregnant women: A repeat measurement-based prospective study. *Environ. Int.* **114**, 12-20 (2018).

12. Jensen, R. C., Glintborg, D., Timmermann, C. A. G., Nielsen, F., Kyhl, H. B., Andersen, H. R., Grandjean, P., Jensen, T. K. & Andersen, M. Perfluoroalkyl substances and glycemic status in pregnant Danish women: the odense child

436 cohort. *Environ. Int.* **116**, 101-107 (2018).
437 13. Lin, C. Y., Chen, P. C., Lin, Y. C. & Lin, L. Y. Association Among Serum
438 Perfluoroalkyl Chemicals, Glucose Homeostasis, and Metabolic Syndrome in
439 Adolescents and Adults. *Diabetes Care* **32**, 702-707 (2008).
440 14. Timmermann, C. A., Rossing, L., Grøntved, A., Ried-Larsen, M., Dalgård, C.,
441 Andersen, L. B., Grandjean, P., Nielsen, F., Svendsen, K. D., Scheike, T. & Jensen,
442 T. K. Adiposity and glycemic control in children exposed to perfluorinated
443 compounds. *J. Clin. Endocrinol. Metab.* **99**, E608-614 (2014).
444 15. Fassler, C. S., Pinney, S. E., Xie, C., Biro, F. M. & Pinney, S. M. Complex
445 relationships between perfluorooctanoate, body mass index, insulin resistance and
446 serum lipids in young girls. *Environ. Res.* **176**, 108558 (2019).
447 16. Khan, S. & Kamal, M, A. Can Wogonin be used in controlling diabetic
448 cardiomyopathy. *Curr. Pharm. Des.* **25,** 2171-2177 (2019).
449 17. Fang, X., Gao, G., Xue, H., Zhang, X. & Wang, H. Exposure of perfluorononanoic
450 acid suppresses the hepatic insulin signal pathway and increases serum glucose in
451 rats. *Toxicology* **294**, 109-115 (2012).
452 18. Zheng, F., Sheng, N., Zhang, H., Yan, S., Zhang, J. & Wang, J. Perfluorooctanoic
453 acid exposure disturbs glucose metabolism in mouse liver. *Toxicol. Appl.*
454 *Pharmacol.* **335**, 41–48 (2007).
455 19. Hines, E. P., White, S. S., Stanko, J. P., Gibbs-Flournoy, E. A., Lau, C. & Fenton,
456 S. E. Phenotypic dichotomy following developmental exposure to
457 perfluorooctanoic acid (PFOA) in female CD-1 mice: low doses induce elevated

458 serum leptin and insulin, and overweight in mid-life☆. *Mol. and Cellular*
459 *Endocrinol.* **304**, 97-105 (2009).
460 20. Lv, Z,, Li, G., Li, Y., Ying, C., Chen, J., Chen, T., Wei, J., Lin, Y., Jiang, Y., Wang,
461 Y., Shu, B., Xu, B. & Xu, S. Glucose and lipid homeostasis in adult rat is impaired
462 by early-life exposure to perfluorooctane sulfonate. *Environ. Toxicol.* **28**, 532-542
463 (2013).
464 21. Yan, S., Zhang, H., Zheng, F., Sheng, N., Guo, X.. & Dai, J. Perfluorooctanoic acid
465 exposure for 28 days affects glucose homeostasis and induces insulin
466 hypersensitivity in mice. *Sci. Rep.* **5**, 11029 (2015).
467 22. Qiu, T., Chen, M., Sun, X., Cao, J., Feng, C., Li, D., Wu, W., Jiang, L. & Yao, X.
468 Perfluorooctane sulfonate-induced insulin resistance is mediated by protein kinase
469 B pathway. *Biochem. Biophys. Res. Commun.* **477**, 781-785 (2016).
470 23. Xu, J., Shimpi, P., Armstrong, L., Salter, D. & Slitt, A. L. PFOS induces
471 adipogenesis and glucose uptake in association with activation of Nrf2 signaling
472 pathway. *Toxicol. Appl. Pharmacol.* **290**, 21-30 (2016).
473 24. Tunaru, S., Bonnavion, R., Brandenburger, I., Preussner, J., Thomas, D., Scholich,
474 K. & Offermanns, S. 20-HETE promotes glucose-stimulated insulin secretion in
475 an autocrine manner through FFAR1. *Nat. Commun.* **9**, 177 (2018).
476 25. Maestri, L., Negri, S., Ferrari, M., Ghittori, S., Fabris, F., Danesino, P. & Imbriani,
477 M. Determination of perfluorooctanoic acid and perfluorooctanesulfonate in
478 human tissues by liquid chromatography/single quadrupole mass spectrometry.
479 *Rapid. Commun. Mass Spectrom.* **20**, 2728–2734 (2006)

480 26. Bodin, J., Groeng, E. C., Andreassen, M., Dirven, H. & Nygaard, U. C. Exposure
481 to perfluoroundecanoic acid (PFUnDA) accelerates insulitis development in a
482 mouse model of type 1 diabetes. *Toxicol. Rep.* **3**, 664-672 (2016).
483 27. Sant, K. E., Jacobs, H. M., Borofski, K. A., Moss, J. B. & Timme-Laragy, A. R.
484 Embryonic exposures to perfluorooctanesulfonic acid (PFOS) disrupt pancreatic
485 organogenesis in the zebrafish, Danio rerio. *Environ. Pollut.* **220**, 807-817 (2017).
486 28. Sant, K. E., Venezia, O. L., Sinno, P. P. & Timme-Laragy, A. R.
487 Perfluorobutanesulfonic acid disrupts pancreatic organogenesis and regulation of
488 lipid metabolism in the zebrafish, Danio rerio. *Toxicol. Sci.* **167**, 258-268 (2019).
489 29. Itoh, Y., Kawamata, Y., Harada, M., Kobayashi, M., Fujii, R., Fukusumi, S., Ogi,
490 K., Hosoya, M., Tanaka, Y., Uejima, H., Tanaka,. H, Maruyama, M., Satoh, R.,
491 Okubo, S., Kizawa, H., Komatsu, H., Matsumura, F., Noguchi, Y., Shinohara, T.,
492 Hinuma, S., Fujisawa, Y. & Fujino, M. Free fatty acids regulate insulin secretion
493 from pancreatic β cells through GPR40. *Nature* **422**, 173-6 (2003).
494 30. Rorsman, P. & Braun, M. Regulation of insulin secretion in human pancreatic
495 islets. *Annu. Rev. Physiol.* **75**, 155-179 (2013).
496 31. Li, C. H., Ren, X. M., Cao, L. Y., Qin, W. P. & Guo, L. H. Investigation of binding
497 and activity of perfluoroalkyl substances to the human peroxisome proliferator-
498 activated receptor beta/delta. *Environ. Sci. Process. Impacts*. **21,**1908-1914 (2019).
499 32. Zhang, L. Y., Ren, X. M., Wan, B. & Guo, L. H. Structure-dependent binding and
500 activation of perfluorinated compounds on human peroxisome proliferator-
501 activated receptor gamma. *Toxicol. Appl. Pharmacol.* **279**, 275-283 (2014).

502 33. Ren, X. M., Zhang, Y. F., Guo, L. H., Qin, Z. F., Lv, Q. Y. & Zhang, L. Y.
503 Structure–activity relations in binding of perfluoroalkyl compounds to human
504 thyroid hormone T3 receptor. *Arch. Toxicol*. **89**, 233-42 (2014).
505 34. Ren, X. M., Qin, W. P., Cao, L. Y., Zhang, J., Yang, Y., Wan, B. & Guo, L.
506 H.Binding interactions of perfluoroalkyl substances with thyroid hormone
507 transport proteins and potential toxicological implications. *Toxicology* **366-367**,
508 32-42 (2016).
509 35. Gao, Y., Li, X. & Guo, L. H. Assessment of Estrogenic Activity of Perfluoroalkyl
510 Acids Based on Ligand-induced Conformation State of Human Estrogen Receptor.
511 *Environ. Sci. & Technol.* **47**, 634-641 (2013).
512 36. Benninghoff, A. D., Bisson, W. H., Koch, D. C., Ehresman, D. J., Kolluri, S. K. &
513 Williams, D. E. Estrogen-like activity of perfluoroalkyl acids in vivo and
514 interaction with human and rainbow trout estrogen receptors in vitro. *Toxicol. Sci.*
515 **120**, 42-58 (2011).
516 37. Xing, J. L., Wang, G., Zhao, J. C., Wang, E. Y., Yin, B. X. Fang, D. S., Zhao, J.
517 X., Zhang, H., Chen, Y. Q. & Chen, W. Toxicity assessment of perfluorooctane
518 sulfonate using acute and subchronic male C57BL/6J mouse models. *Environ.*
519 *Pollution* **210**, 388e396 (2016).
520 38. Niu, B., Su, H., Xia, X. S., He, Q., Xue, Y. M. & Yan, X. M. The role of interleukin-
521 1beta and extracellular signal-regulated kinase 1/2 in glucose-stimulated insulin
522 secretion. *Kaohsiung J. Med. Sci.* **33**, 224-228, (2017).
523 39. Cao, L. Y., Ren, X. M., Li, C. H., Zhang, J., Qin, W. P., Yang, Y., Wan, B. & Guo,

L. H. Bisphenol AF and Bisphenol B Exert Higher Estrogenic Effects than Bisphenol A via G Protein-Coupled Estrogen Receptor Pathway. *Environ. Sci. Technol.* **51**, 11423-11430 (2017).

40. Ren, X. M., Cao, L. Y., Zhang, J., Qin, W. P., Yang, Y., Wan, B. & Guo, L. H. Investigation of the binding interaction of fatty acids with human G protein-coupled receptor 40 using a site-specific fluorescence probe by flow cytometry. *Biochemistry* **55**, 1989-1996 (2016).
41. Le-May, C., Chu, K., Hu, M., Ortega, C. S., Simpson, E. R., Korach, K. S., Tsai, M. J. & Mauvais-Jarvis, F. Estrogens protect pancreatic beta-cells from apoptosis and prevent insulin-deficient diabetes mellitus in mice. *Proc. Natl. Acad. Sci. USA* **103**, 9232-9237 (2006).
42. Liu, S., Le-May, C., Wong, W. P., Ward, R. D., Clegg, D. J., Marcelli, M., Korach, K. S. & Mauvais-Jarvis, F. Importance of extranuclear estrogen receptor-alpha and membrane G protein-coupled estrogen receptor in pancreatic islet survival. *Diabetes* **58**, 2292-2302 (2009).
43. Balhuizen, A., Kumar, R., Amisten, S., Lundquist, I. & Salehi, A. Activation of G protein-coupled receptor 30 modulates hormone secretion and counteracts cytokine-induced apoptosis in pancreatic islets of female mice. *Mol. Cell. Endocrinol.* **320**, 16-24 (2010).
44. Cho, J. H., Lee, K. M., Lee, Y. I., Nam, H. G. & Jeon, W. B. Glutamate decarboxylase 67 contributes to compensatory insulin secretion in aged pancreatic islets. *Islets* **11**, 33-43 (2019).

546 45. Minami, K., Yano, H., Miki, T., Nagashima, K., Wang, C. Z., Tanaka, H.,
547 Miyazaki, J. I. & Seino, S. Insulin secretion and differential gene expression in
548 glucose-responsive and -unresponsive MIN6 sublines. *Am. J. Physiol. Endocrinol.*
549 *Metab.* **279**, E773–E781 (2000).
550 46. Ishihara, H., Asano, T., Tsukuda, K., Katagiri, H., Inukai, K., Anai, M., Kikuchi,
551 M., Yazaki, Y., Miyazaki, J. I. & Oka, Y. Pancreatic beta cell line MIN6 exhibits
552 characteristics of glucose metabolism and glucose-stimulated insulin secretion
553 similar to those of normal islets. *Diabetologia* **36**, 1139-1145 (1993).
554 47. Klimek, K., Benko, A., Pałka, K., Ludwiczuk, A. & Ginalska, G. Ion-exchanging
555 dialysis as an effective method for protein entrapment in curdlan hydrogel. *Mater.*
556 *Sci. Eng. C Mater. Biol. Appl.* **105**, 110025 (2019).
557 48. Li, L., Song, G. W. & Xu, Z. S. Study on the interaction between bovine serum
558 albumin and potassium perfluorooctane sulfonate. *J. Dispers. Sci. Technol.* **31**,
559 1547-1551 (2010).
560 49. Chen, H., He, P., Rao, H., Wang, F., Liu, H. & Yao, J. Systematic investigation of
561 the toxic mechanism of PFOA and PFOS on bovine serum albumin by
562 spectroscopic and molecular modeling. *Chemosphere* **129**, 217-224 (2015).
563 50. Wang, Y., Zhang, H., Kang, Y. & Cao, J. Effects of perfluorooctane sulfonate on
564 the conformation and activity of bovine serum albumin. *J. Photochem. Photobiol.*
565 *B.* **159**, 66-73 (2016).
566 51. Ashcroft, F. M., Proks, P., Smith, P. A., Ammala, C., Bokvist, K. & Rorsman, P.
567 Stimulus-secretion coupling in pancreatic beta cells. *J. Cell. Biochem.* **55**, 54-65

(1994).

52. Ghislain, J. & Poitout, V. The Role and Future of FFA1 as a Therapeutic Target. *Handb. Exp. Phamacol.* **236**, 159-180 (2016).

53. Fujimoto, S., Mizuno, R., Saito, Y. & Nakamura, S. Clinical application of wave intensity for the treatment of essential hypertension. *Heart Vessels.* **19**, 19-22 (2004).

54. Tsujihata, Y., Ito, R., Suzuki, M., Harada, A., Negoro, N., Yasuma, T., Momose, Y. & Takeuchi, K. TAK-875, an orally available G protein-coupled receptor 40/free fatty acid receptor 1 agonist, enhances glucose-dependent insulin secretion and improves both postprandial and fasting hyperglycemia in type 2 diabetic rats. *J. Pharmacol. Exp. Ther.* **339**, 228-237 (2011).

55. Hu, H., He, L. Y., Gong, Z., Li, N., Lu, Y. N., Zhai, Q. W., Liu, H., Jiang, H. L., Zhu, W. L. & Wang, H. Y. A novel class of antagonists for the FFAs receptor GPR40. *Biochem. Biophys. Res. Commun.* **390,** 557–563 (2009).

56. Briscoe, C. P., Peat, A. J., McKeown, S. C., Corbett, D. F., Goetz, A. S., Littleton, T. R., McCoy, D. C., Kenakin, T. P., Andrews, J. L., Ammala, C., Fornwald, J. A., Ignar, D. M & Jenkinson, S. Pharmacological regulation of insulin secretion in MIN6 cells through the fatty acid receptor GPR40: identification of agonist and antagonist small molecules. *Br. J. Pharmacol.* **148**, 619-628 (2006).

57. Srivastava, A., Yano, J., Hirozane, Y., Kefala, G., Gruswitz, F., Snell, G., Lane, W., Ivetac, A., Aertgeerts, K., Nguyen, J., Jennings, A. & Okada, K. High-resolution structure of the human GPR40 receptor bound to allosteric agonist TAK-

875. *Nature* **513**, 124-127 (2014).

58. Zhang, L. Y., Zhu, X. J. & Xu, J. X. Binding and activation of G protein-coupled receptor 40 by perfluorodecanoic acid. *J. Environ. Appl. Biores.* **05**, 16-19 (2017).

59. Zhang, L. Y., Ren, X. M. & Guo, L. H. Structure-based investigation on the interaction of perfluorinated compounds with human liver fatty acid binding protein. *Environ. Sci. Technol.* **47**, 11293-11301 (2013).

60. Weiss, J. M., Andersson, P. L., Lamoree, M. H., Leonards, P. E., van Leeuwen, S. P. & Hamers, T. Competitive binding of poly- and perfluorinated compounds to the thyroid hormone transport protein transthyretin. *Toxicol. Sci.* **109**, 206-216 (2009).

603

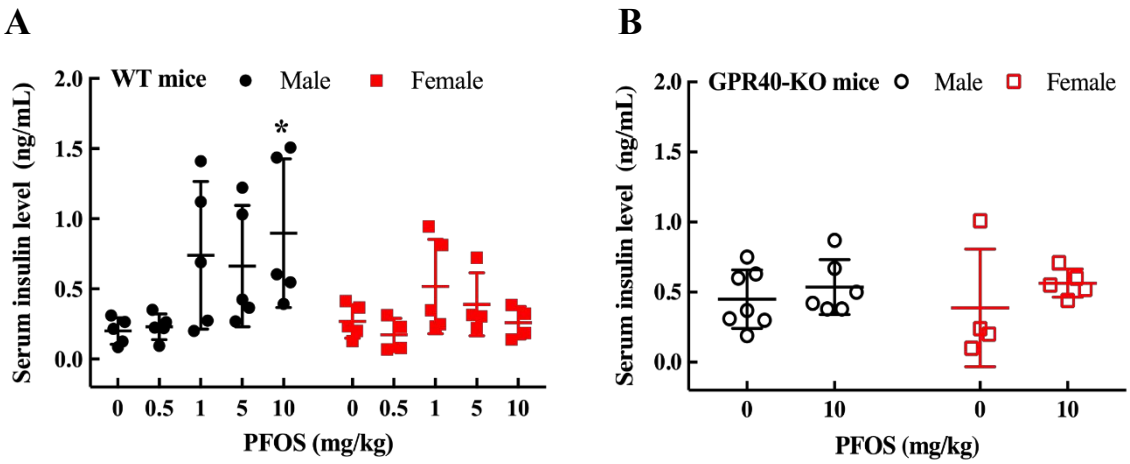

604 **Figure 1** Effects of PFOS on the fasting insulin level of wild type (WT) and GPR40
605 knock out (GPR40-KO) mice. Fasting serum levels of WT mice (**A**) and GPR40-KO
606 mice (**B**) after administration of PFOS for one hour. * means $p < 0.05$, compared with
607 solvent control of each group (0 mg/kg, 0.5% methyl cellulose and 0.5% dimethyl
608 sulfoxide).

609

610

611

612

613

614

615

616

617

618

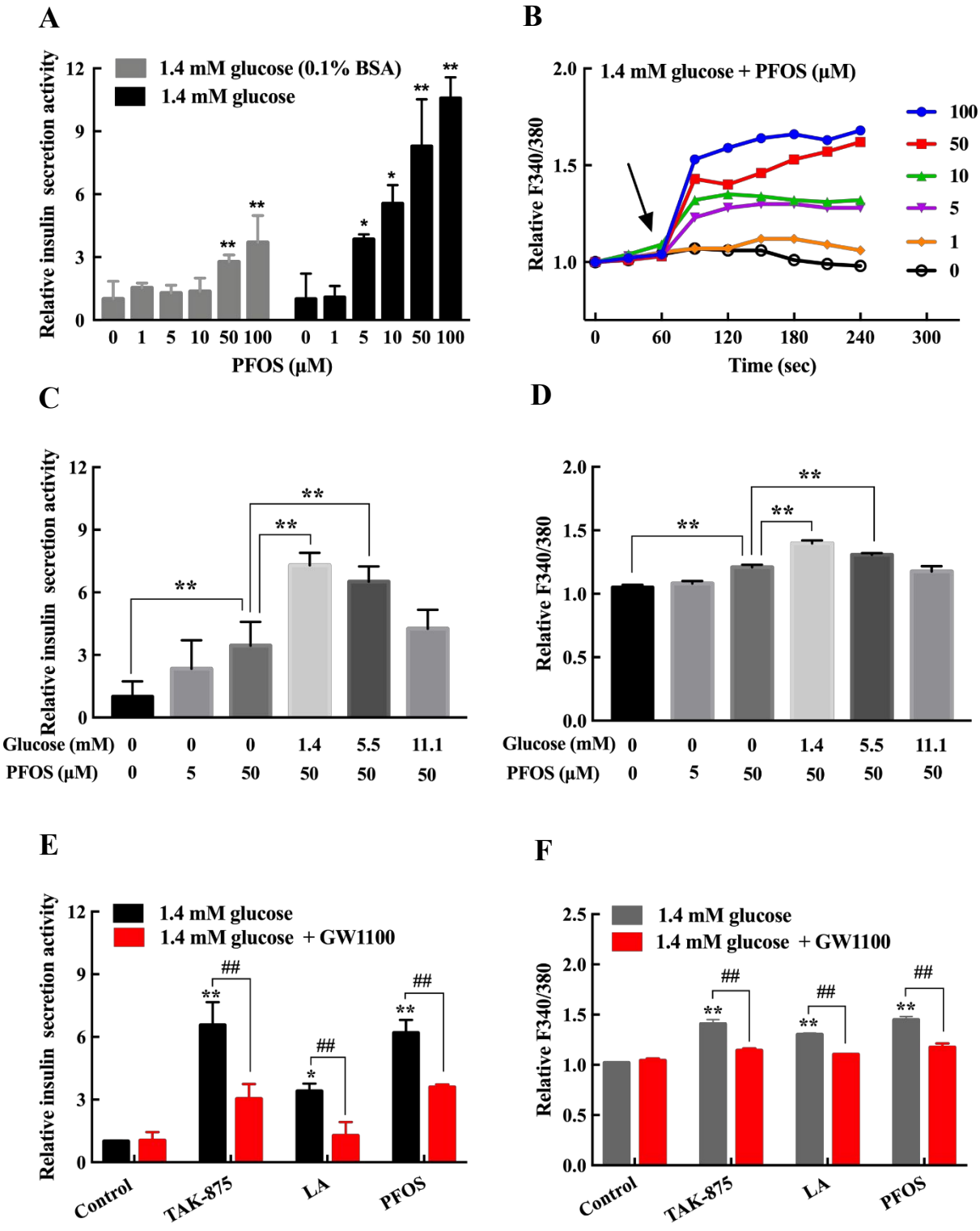

Figure 2 Effects of PFOS on the insulin secretion activity (A, C, E) and intracellular calcium level (B, D, F) of β-TC-6 cells and the inhibitory effects of GW1100. (**A**) Effects of different concentration of PFOS on the insulin secretion activity of β-TC-6

622 cells in presence of 1.4 mM glucose, with or without 0.1% BSA in the KRBH buffer.
623 (**B**) Effects of different concentration of PFOS on intracellular calcium level of β-TC-
624 6 cells in the presence of 1.4 mM glucose. (**C, D**) Effects of 5 μM and 50 μM PFOS on
625 the insulin secretion activity and intracellular calcium level of β-TC-6 cells in the
626 absence of glucose, and the effects of 50 μM PFOS on the insulin secretion activity and
627 intracellular calcium level of β-TC-6 cells in the presence of different concentration of
628 glucose. (**E, F**) Effects of 10 μM TAK-875, 250 μM lauric acid (LA) and 50 μM PFOS
629 on the insulin secretion activity and intracellular calcium level of β-TC-6 cells in the
630 presence of 1.4 mM glucose, and the inhibitory effects of 10 μM GW1100 on them. *
631 means $p < 0.05$ and ** means $p < 0.01$, compared with the corresponding control group,
632 ## means $p < 0.01$ compared with the groups not pre-treated with GW1100.
633

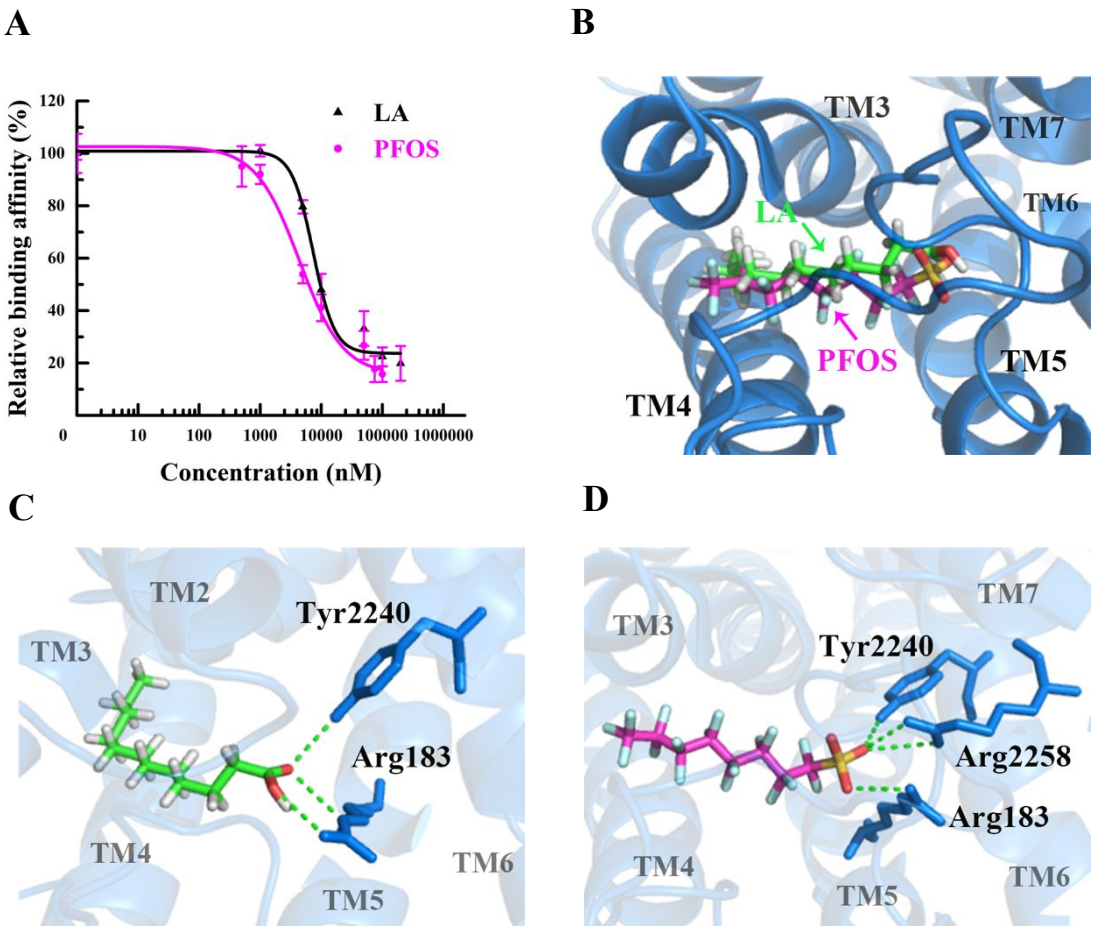

634 **Figure 3** Studies of the interactions of lauric acid (LA) and PFOS with human GPR40
635 by competitive binding assay and molecular docking. (**A**) Competitive binding curves
636 of LA and PFOS with human GPR40. (**B**) Molecular docking simulation of LA and
637 PFOS into the binding pocket of human GPR40. (**C, D**) Interactions of LA (**C**) and
638 PFOS (**D**) with amino acid residues of GPR40. LA and PFOS are shown as stick (C:
639 magenta or green, F: cyan, S: yellow, O: red, H: white); GPR40 is shown as marine-
640 blue helix; amino acid residues of GPR40 are shown as marine-blue stick and hydrogen
641 bonds are indicated by green dotted lines.

642

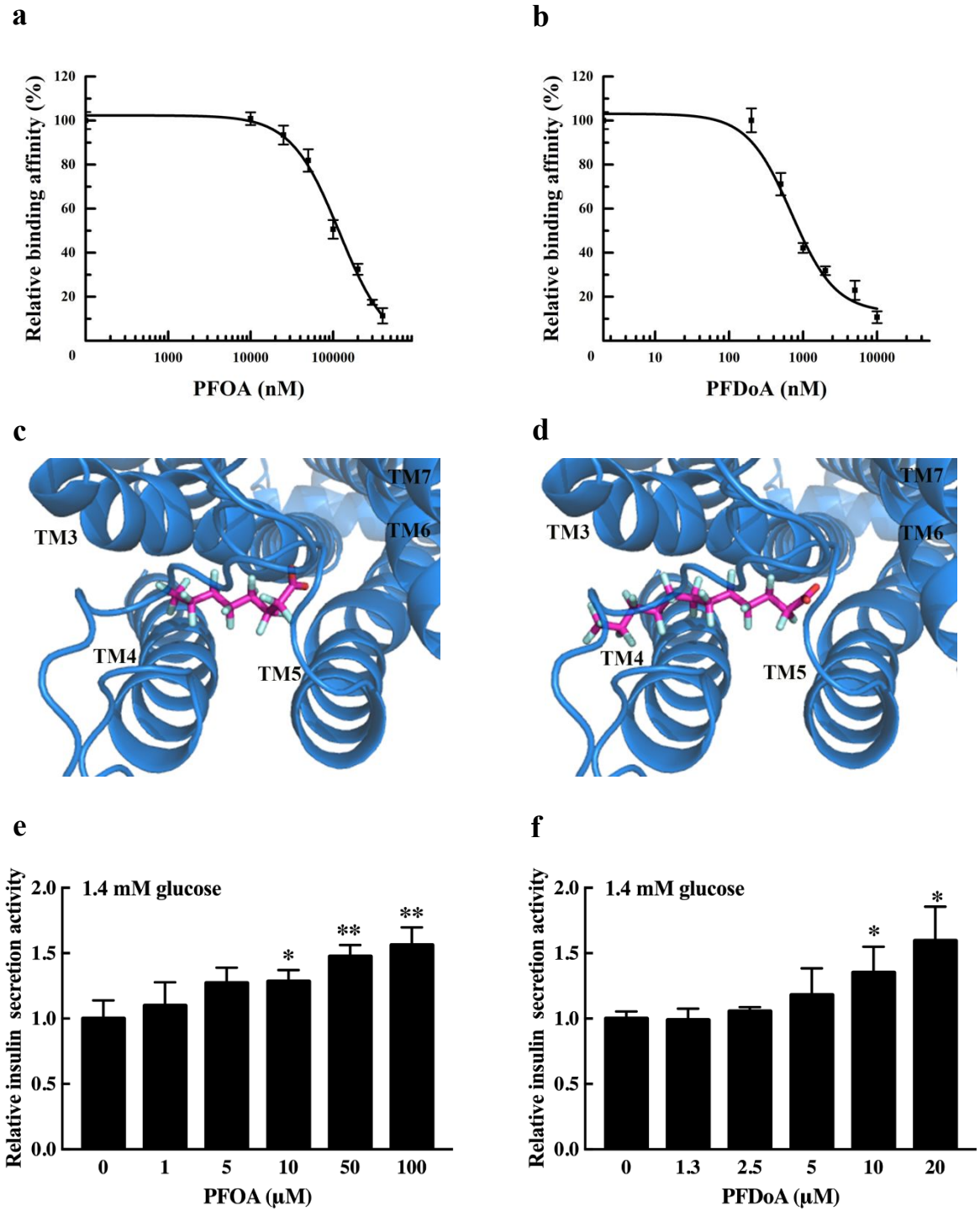

643 **Figure 4** Predictions of the insulin-secretion disruption risks of PFOA and PFDoA via

644 GPR40 pathway. (**A, B**) Competitive binding curves of PFOA and PFDoA with human

645 GPR40. (**C, D**) Molecular docking analysis of PFOA and PFDoA to human GPR40.

646 (**E, F**) Effects of PFOA and PFDoA on the insulin secretion activity of β-TC-6 cells in

647 the present of 1.4 mM glucose. * means $p < 0.05$, ** means $p < 0.01$, compared with

648 the control group (0.1% DMSO).

649

650

651 **Table 1** Abbreviation (Abbre.), highest tested concentration (HTC), half inhibitory
652 concentration (IC_{50}), relative binding affinity (RBA) values, and docking results of
653 lauric acid (LA), TAK-875 and 15 PFASs with human GPR40.

Compound	Abbre.	HTC (μM)	IC_{50} (μM)	RBA	Hydrogen bond
$C_{12}H_{24}O_2$	LA	200	7.4±0.6	1	Arg183, Tyr2240
$C_{29}H_{32}O_7S$	TAK-875	2	< 0.1	616.7	Arg183, Arg2258
$C_4HF_7O_2$	PFBA	400	ND	ND	Arg183, Arg2258
$C_4HF_9O_3S$	PFBS	400	ND	ND	Tyr 2240
$C_6HF_{11}O_2$	PFHxA	400	ND	ND	Tyr 2240, Arg2258
$C_6HF_{13}O_3S$	PFHxS	400	167.7±9.8	< 0.1	Arg183, Arg2258
$C_7HF_{13}O_2$	PFHpA	400	ND	ND	Tyr 2240, Arg2258
$C_8HF_{15}O_2$	PFOA	400	119.3±19.3	0.1	Arg183, Tyr2240, Arg2258
$C_8HF_{17}O_3S$	PFOS	100	4.4±0.7	1.7	Arg183, Tyr2240, Arg2258
$C_9HF_{17}O_2$	PFNA	100	24.3±18.5	0.3	Arg183, Tyr2240, Arg2258
$C_{10}HF_{19}O_2$	PFDA	50	5.0±1.0	1.5	Tyr2240, Arg2258
$C_{11}HF_{21}O_2$	PFUnA	10	2.9±0.6	2.6	Tyr2240, Arg2258
$C_{12}HF_{23}O_2$	PFDoA	10	0.7±0.1	10.6	Tyr2240, Arg2258
$C_{13}HF_{25}O_2$	PFTriDA	10	ND	ND	Tyr2240, Arg2258
$C_{14}HF_{27}O_2$	PFTeDA	10	ND	ND	Arg183, Tyr2240
$C_{16}HF_{31}O_2$	PFHxDA	10	ND	ND	Arg183, Tyr2240, Arg2258
$C_{18}HF_{35}O_2$	PFOcDA	10	ND	ND	Tyr2240

654
655
656
657